

Design and Experimental Study of an Implemented Solar Air Heater Destined for Red Algae Drying

Fatima Chanaa*, Rachid Bendaoud*, Said Bounouar*, Charaf Hajjaj*, Abderrahim El-abidi**, Hassan Ezzaki*, Abdelhaq El Rhassouli***, Rédouane Rmaily*, Mohammadi Benhmida*‡

* Laboratory of Electronics, Instrumentation and Energetic, Department of physics, Chouaïb Doukkali University, El Jadida, Morocco

** Laboratory of Materials, Processes, Environment and Quality, the National School of Applied Sciences, Cadi Ayyad University, Safi, Morocco

***Lycée Technique Louis Aragon, Academy of Franch-Comté, Héricourt, France

(chanaa.f@ucd.ac.ma, rbendaoud27@gmail.com, bounouar.said@gmail.com, hajjaj.charaf@gmail.com, a.elabidi@uca.ma, ezzaki.hassan@gmail.com, rhassouli@wanadoo.fr, rrmaily@yahoo.fr, benhmida@gmail.com)

‡ Corresponding Author; Mohammadi Benhmida, Route Ben Maachou B.P 20, 24000, El Jadida, Morocco

Tel: +212 6 82 08 04 75, Fax: +212 6 69 82 84 06, benhmida@gmail.com

Received: 24.10.2018 Accepted:04.12.2018

Abstract- An experimental study is carried out on an affordable cost air heater with a constant volumetric airflow of 0.015 kg/s m^2 , under sunlight in a coastal area. It is a single pass solar air heater with glazing and corrugated sheet metal absorber locally manufactured and destined for red algae *Gelidium sesquipedale* drying. The heater is continuously maintained towards the sun in order to increase the absorbed energy. Solar irradiance, inlet and outlet air temperature of the solar heater, as well as the average temperature at the absorber surface are measured. Special care is taken to airflow measurements. The effect of collector tilt angle on its thermal and effective performances is characterized. For a tilt angle of 60° and under an average irradiance of 811 W/m^2 during 9 hours of exposure, 3 kWh/m^2 are harvested, with an efficiency of 41.2% and a temperature rise of 22°C . The corresponding specific power is 337 W/m^2 , which is about 14.7 times the power of the used draft fan. The outlet air temperature is in the range of 34 to 58°C which significantly reduces the drying time of red algae *Gelidium sesquipedale* compared to the traditional drying process at approximately 28°C .

Keywords Solar air heater, *Gelidium sesquipedale*, corrugated sheet absorber, thermal efficiency, tilt angle impact.

1. Introduction

In order to improve the performance of solar air heating collectors, a variety of design, materials and flow configurations are proposed in several studies [1-5]. The major objectives are: reducing losses, maximizing the converted energy in the absorber, and transferring more energy to the airflow. This last action is the major field of solar air heaters improvement and is the focus of most studies. It can be achieved by either extending the heat exchange surface or by increasing the velocity and turbulence of airflow.

Extending the heat exchange surface could be achieved by using corrugated absorbers [6,7]. Karim and Hawlader [8] carried out an experimental and theoretical study on the performance of a flat plate, finned and v-corrugated solar air heater. They concluded that the corrugated absorber is more efficient compared to the flat plate heater with an increase in thermal efficiency of 10-15% and 5-11% in single and double passage modes, respectively.

The increase of local air velocity and turbulence is often achieved by creating an artificial roughness consisting of obstacles of various shapes and sizes placed in different configurations [9-12]. Moumami et al. [13] used a system of rectangular obstacles fixed in the bottom plate of the flow conduit perpendicular to the airflow. The experimental

results show that the used system improves the efficiency of 35% compared to the heater without obstacles. However, as presented by Bhushan and Singh in their review [14], the use of artificial roughness produces a significant improvement in thermal efficiency on one hand, and a disproportionate increase in the friction losses on the other hand. Therefore, an increase of consumed electrical energy by unit of thermal energy produced is observed.

Using absorbers made of porous materials is another technique to increase both the surface exchange and air turbulence [15-17] in order to enhance heat transfer to airflow. Ahmad et al. [18] carried out an experimental study to determine the design parameters of packed-bed solar air heaters by examining the effect of the depth and porosity of matrices on the performance of such systems. The study shows that the thermo-hydraulic efficiency improvement, compared to the smooth collector one, is only available in a relatively narrow range of operating conditions due to significant pressure drop, which is not the case for the thermal efficiency.

The use of these techniques to improve the thermal performance of the collector can be considered effective if the ratio of additional energy harvested to the additional electrical energy consumed is equal or more than that of initial operating condition.

This paper presents an experimental study of a single flow corrugated solar air heater, manufactured locally using affordable cost materials. The objective of this study is to investigate the air heater characteristic parameters and its energetic performance for different tilt angles. A manual tracking along a vertical axis using a removable carriage is performed to increase the energy harvested. The experiments were conducted under sunlight with fixed airflow at El Jadida (33°15' North, 8°30' West), which is a coastal region with average moisture of 65% and annual solar irradiance of 5600 Wh/m²/day [19-23]. The heater is destined for *Gelidium sesquipedale* drying, the most exploited red algae species in El Jadida [24] which is an excellent source of agar-agar [25-26], a product with gelation power [27] and interesting several industrial sectors (agrifood,

biotechnology, pharmacology, medicine, cosmetology, etc) [28-30].

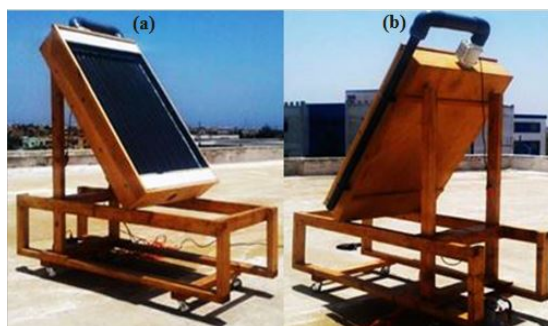


Fig. 1. Solar air heater: (a) face side, (b) back side.

2. Materials and Methods

2.1. Experimental device description

The studied solar air heater is a single flow and single glazed collector with a capture surface of 1m² (Fig. 1 and Fig. 2). It is composed of:

- a solid wood case covered with an insulating layer of polystyrene 4 cm thick, and equipped with two perforated barriers containing 11 holes for having a good airflow distribution, therefore improving the heat transfer by convection [31].
- an absorber made of corrugated and galvanized steel sheet, 0.3 mm thick. Its front face is covered with a layer of matte black paint.
- an ordinary glass pane, 4 mm thick.
- an air gap of 7 cm separates the glass from the absorber.
- a fan placed downstream of the collector.

The system is sealed with silicone and tape. A removable wooden trolley is used to facilitate the movement and the orientation of the air heater.

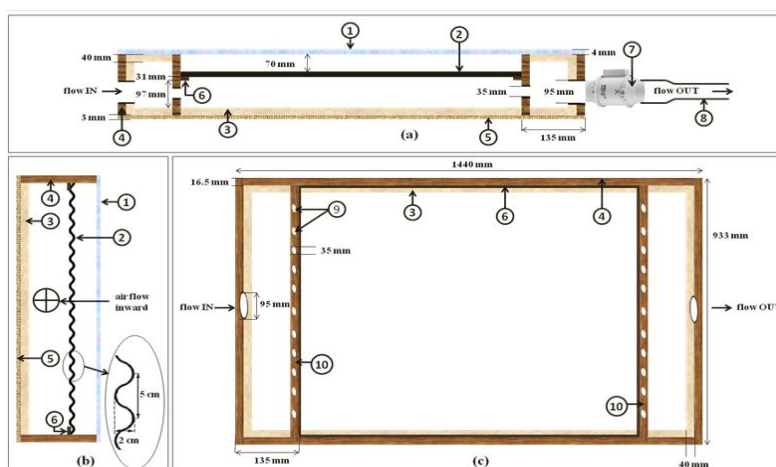


Fig. 2. Solar air heater: (a) longitudinal, (b) transverse, and (c) horizontal cross sections. transparent cover (1), corrugated absorber (2), insulation (3), wooden chest (4), plywood (5), absorber support (6), fan (7), tube (8), holes (9), perforated barrier (10).

2.2. Measurement methods

Measurements are carried out under sunlight with a constant volumetric airflow of 0.015 kg/s m² (42 Nm³/h m² at Normal Condition of Temperature and Pressure: P = 1atm, T = 0°C). The collector is manually maintained towards the sun. The air is admitted into the collector at ambient temperature. The first series of measurements were carried out by June with tilt angles from the horizontal plane ($\theta = 0^\circ$), to $\theta = 25^\circ$ and $\theta = 33^\circ$. Two other series of measurements were conducted by July with tilt angles of $\theta = 60^\circ$ and 90° . Measurements were started after one operating hour of the system.

The measured parameters are inlet (T_{in}) and outlet (T_{out}) air temperatures, temperature at the absorber front surface (T_{abs}), volumetric airflow (q_v), and global tilted solar irradiance (G) (Table 1).

During the experiments, the solar collector was directed towards the sun using a removable carriage. Adjustments were done manually every 10 min.

To determine T_{abs} , the absorber surface was divided into 20 zones along 4 lines (A, B, C, D) and 5 columns. Due to the symmetry of the collector, measurements were done at 12 points (Fig. 3).

At the fan output, the air is brought through a pipe with smaller diameter than the fan outlet one (Fig. 4). This is in order to have a sufficiently high speed and dynamic pressure, far from the detection thresholds of the used Pitot tube and differential pressure gauge. Measuring section location is chosen in such a way that the straight lengths are equal to 20 times the tube diameter upstream of the measurement section, and 5 times the tube diameter downstream of the measurement section (Fig. 4). This is so that the velocity profile is more regular.

Table 1. Experimental measurements and used devices

Measured parameter	Measuring frequency	Measuring device	Uncertainty (± % reading)
T_{in} (°C)	5 min	Thermocouple type K	± 2%
T_{out} (°C)	5 min	Thermocouple type K	± 2%
T_{abs} (°C)	10 to 15 min depending on the measurement duration	Removable rod equipped with a thermocouple type K	± 2%
q_v (kg/s m ²)	15 to 20 min depending on the measurement duration	Pitot tube of 3 mm with differential pressure gauge (Extech HD350)	± 2%
G (W/m ²)	Record of the average value over 5 min, every 5 min	Solarimeter KIMO SL 200, placed parallel to the illuminated side of the collector	± 5%

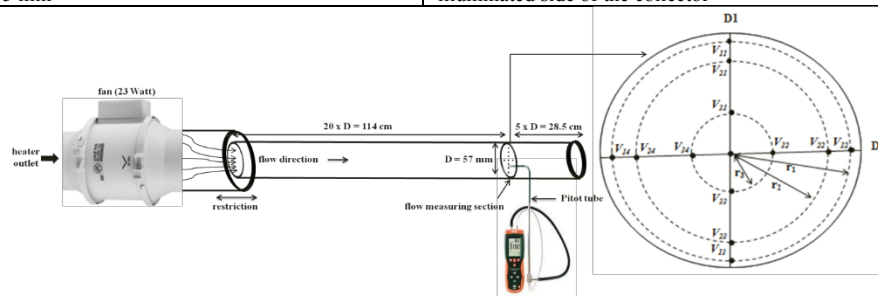


Fig. 4. Measurement points across the tube section according to Gauss exploration method.

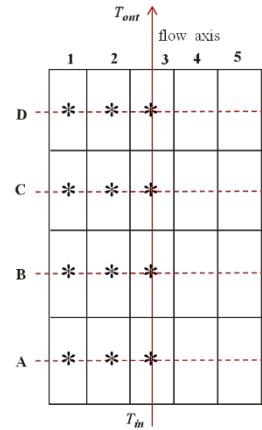


Fig. 3. Temperature measurement points on the absorber surface T_{abs} (*).

The volumetric airflow rate (q_v) is deduced from the velocity field exploration. Velocity measurement points were determined using Gauss exploration method [32]. Measurements were made along two perpendicular diameters (D1, D2), at 3 point per radius (r_1, r_2, r_3), i.e. 12 points (Fig. 4). Velocity measurement points are shown in Table 2.

Table 2. Velocity measurement points and weighting coefficient

Number of measurement points per radius	Relative radius r_n / R Radius referred to the radius R of the pipe ($R = 2.85 \text{ cm}$)	Weighting coefficient C_n
3	$r_1/R = 0.942$	$C_1 = 0.278$
	$r_2/R = 0.707$	$C_2 = 0.444$
	$r_3/R = 0.336$	$C_3 = 0.278$

The volumetric airflow is determined as follows [32]:

$$q_v = \pi R^2 \sum_{n=1}^3 V_{mean.n} C_n \quad (1)$$

where $V_{mean.n}$ denotes the average air velocity on the radius n ($n = 1, 2, 3$). So that on the radius [32]:

$$\begin{cases} r_1 : V_{mean.1} = (V_{11} + V_{12} + V_{13} + V_{14})/4 \\ r_2 : V_{mean.2} = (V_{21} + V_{22} + V_{23} + V_{24})/4 \\ r_3 : V_{mean.3} = (V_{31} + V_{32} + V_{33} + V_{34})/4 \end{cases} \quad (2)$$

Instantaneous thermal efficiency (η) of the solar air heater is defined as the ratio of the useful recovered energy ($Q_u = \rho q_v C_p (T_{out} - T_{in})$) to the amount of total solar energy incident on the heater surface (A_c) as reported in Kabeel et al. [33] and Chabane et al. [34]:

$$\eta = \frac{\rho q_v C_p (T_{out} - T_{in})}{A_c G} \quad (3)$$

where: ρ - air density (kg/m^3); C_p - air specific heat (J/kg K).

The effective efficiency (η_{eff}) of the air heater is evaluated on the basis of net energy extracted from the collector which corresponds to the difference between the useful heat gain and the electrical consumption of the fan necessary for air circulation inside the collector. The following expression for effective efficiency was used in the present analysis.

$$\eta_{eff} = \frac{Q_u - P_{elec.fan}}{A_c G} \quad (4)$$

where $P_{elec.fan}$ is the fan electrical power required to force air through the collector.

3. Results and discussion

3.1. Airflow rate and flow regime

The average flow rate obtained for the three series of measurements is of 0.015 kg/s m^2 , with a standard deviation of 0.001 kg/s m^2 (Table 3), which produces a laminar flow with a Reynolds number of 1805.

Table 3. Average flow rate and standard deviation obtained for the three measurement series

Series N°	Average flow rate kg/s m^2	Number of measurements	Standard deviation kg/s m^2
1	0.0153	10	0.0014
2	0.0150	11	0.0009
3	0.0148	22	0.0010
Average	0.0150	43	0.0011

Fig. 5 shows some measurements of velocity fields V (m/s) following two diameters (D1, D2) of measurement section. The velocity profiles along D1 and D2 are very close but not superimposed as expected in the case of a fully established and permanent regime. The differences observed are essentially due to the instability of the flow regime. That is supported by the temperature measurement on the absorber surface. Indeed, these temperatures are almost constant on each of A,B,C,D lines perpendicular to the airflow direction, as shown on table 4, which indicates a plug flow that is not yet fully established in the duct of the collector.

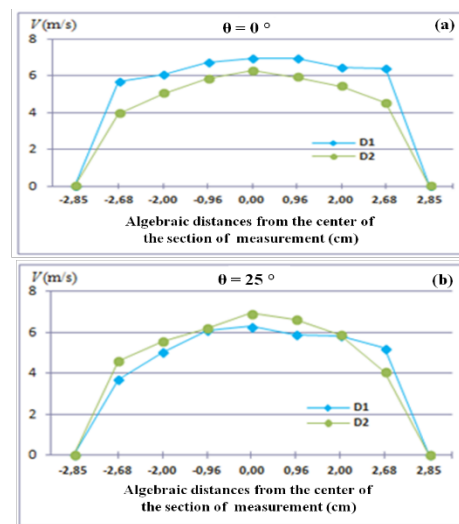


Fig. 5. Airflow velocity profiles along diameters D1 and D2 of the measuring section, for tilt angles of: (a) $\theta = 0^\circ$, (b) $\theta = 25^\circ$ (series 1).

Table 4. Examples of temperature measurements (series 1) carried out on the absorber surface (Fig. 3) for tilt angles: (a) $\theta = 0^\circ$, (b) $\theta = 33^\circ$

(a)	$\theta = 0^\circ / G = 1000 \text{ W/m}^2$		
	$T_{abs} (^\circ\text{C})$		
	Column 1	Column 2	Column 3
Line D	102	102	101
Line C	97	96	97
Line B	92	91	89
Line A	81	79	80

(b)	$\theta = 33^\circ / G = 917 \text{ W/m}^2$		
	$T_{abs} (^\circ\text{C})$		
	Column 1	Column 2	Column 3
Line D	86	86	86
Line C	82	82	82
Line B	75	74	76
Line A	70	69	71

3.2. Influence of the air heater tilt angle

Table 5 shows for each measurement series tilt angle θ used and mean, minimum and maximum irradiance. The corresponding performance is described by four parameters: the air temperature rise ($\Delta T = T_{out} - T_{in}$), $\Delta T/G$, η and η_{eff} .

The overall results from the three measurements series show an increase of $\Delta T/G$ and η with an increase of θ from 0° to 90° (Table 5). That can be explained by more convective heat transfer between the absorber underside and the airflow for more upright angles, mainly for laminar flow with low Reynolds number. This heat transfer contributes also to cooling the absorber and consequently to less losses. Chabane et al. [35] found similar results in an experimental study where they investigated the effect of tilt angle onto the thermal performance of a single pass solar air heater and showed that the collector efficiency is higher for $\theta = 60^\circ$ than that for $\theta = 0^\circ$. In an analytical study conducted by Dilip and Rajeev [36], the performance of a solar air heater for grain

Table 5. Results of the three measurement series

Series N°	Tilt angle θ in degrees	Solar irradiance G (W/m^2)		Air temperature rise ΔT ($^{\circ}C$)		Average $\Delta T/G$ ($^{\circ}C/Wm^{-2}$)	Average thermal efficiency η_a (%)	Average effective efficiency η_{eff} (%)
		Range: Min. Max.	Average	Average	Max.			
1	0	989 – 1002	995	14.0	15.2	0.0141	21.9	19.6
	25	825 – 1050	1002	17.2	18.7	0.0172	26.5	24.2
	33	610 – 1068	806	17.0	19.8	0.0214	33.1	30.2
2	60	182 – 0988	811	22.2	29.1	0.0271	41.2	38.0
3	90	096 – 0864	541	15.0	25.1	0.0270	42.2	38.4

drying was evaluated and they conclude that the grain temperature increases as the collector tilt angle increases.

The thermal and effective efficiencies are quite similar because the fan consumption and pressure drop throughout the heater are low. El-abidi et al [31] conducted a 3D simulation with finite element model of a modified simple back-pass solar collector in order to predict parameters influencing its thermal performances, such as the number of perforations in the configuration. They highlighted that barriers containing 11 holes, the case of our study, generate only a small pressure drop of about 10 Pa, while those of barriers containing 7 and 5 perforations generate losses of about 22 and 30 Pa respectively.

Series 2 with $\theta = 60^{\circ}$, and series 3 with $\theta = 90^{\circ}$ show similar η and $\Delta T/G$ values (Table 5).

For the tilt angle of 60° and under an average irradiance of $811 W/m^2$ during 9 hours of exposure (from 10:55 AM to 8:10 PM), 3 kWh were harvested, with a mean heat power of 337 W. The corresponding average values of η , ΔT and $\Delta T/G$, are of 41.2%, 22 $^{\circ}C$ and 0,0271 $^{\circ}C/Wm^{-2}$ respectively.

3.3. Air temperature rise and efficiency evolution with irradiance

Fig. 6 shows linear increase of ΔT as a function of G and the regression lines pass by the origin point. Thus, for a given θ and q_v correspond a slope K_{θ,q_v} which can be considered as a characteristic parameter of the system.

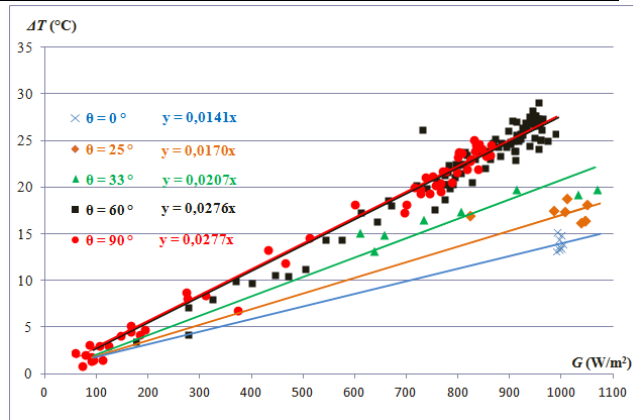


Fig. 6. Variation of ΔT as a function of G for the three experiments series.

Fig. 7 and Fig. 8 show the evolution of η and G as a function of time for measurement series 2 and 3. Although G varies widely on a large interval along time scale, η remains quasi-constant with slight oscillations around averages values of 41.2%, and 42.2%, for the both measurement series 2 and 3, respectively. Similar results have been reported in literature [37,38].

For fast variations of G , dramatic oscillations of η were recorded. Indeed, although that G and ΔT vary in the same direction, they don't vary in the same proportions. ΔT is related to heat capacity of the collector which is time dependent, while G can vary rapidly following weather conditions. Thus, when G increases rapidly, the corresponding ΔT remains relatively low. Consequently, the ratio of ΔT to G (proportional to η) decreases and vice versa.

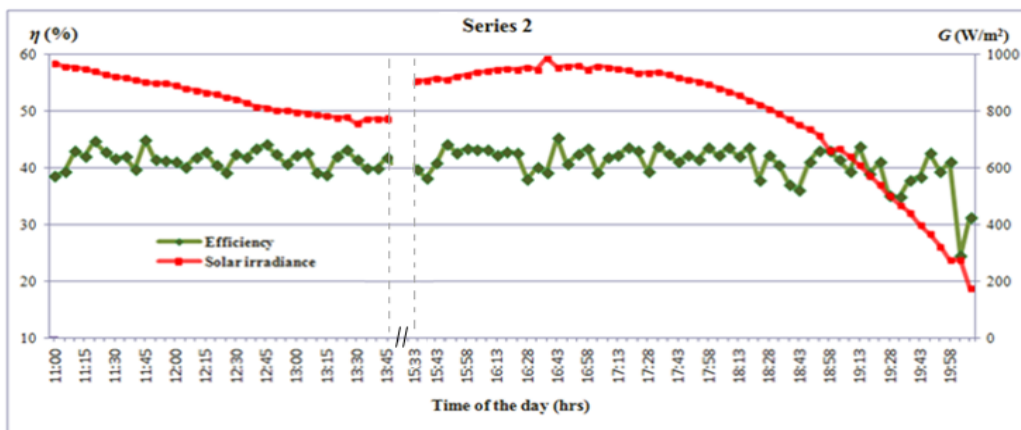


Fig. 7. Measurement series 2 ($\theta = 60^\circ$). Variation of η and G as a function of time.

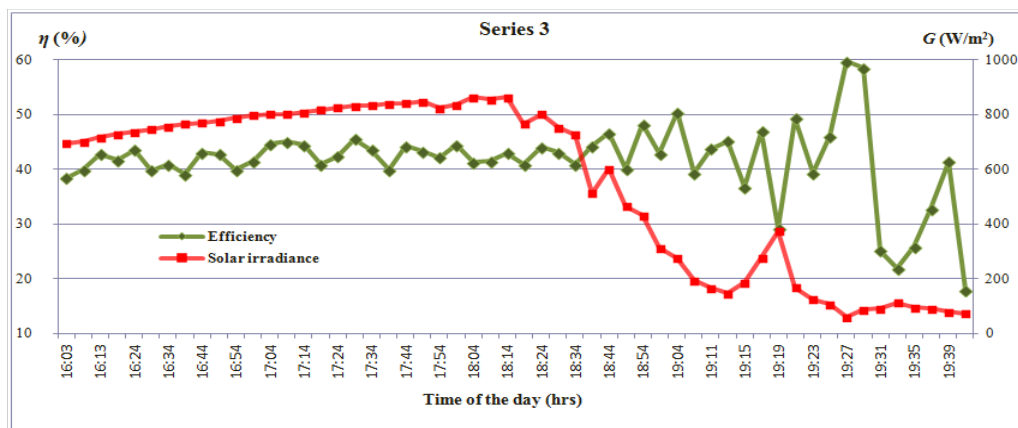


Fig. 8. Measurement series 3 ($\theta = 90^\circ$). Variation of η and G as a function of time.

Fig. 9. Variation of η as a function of $\Delta T/G$ for the three measurement series.

3.4. Evolution of the efficiency with $\Delta T/G$

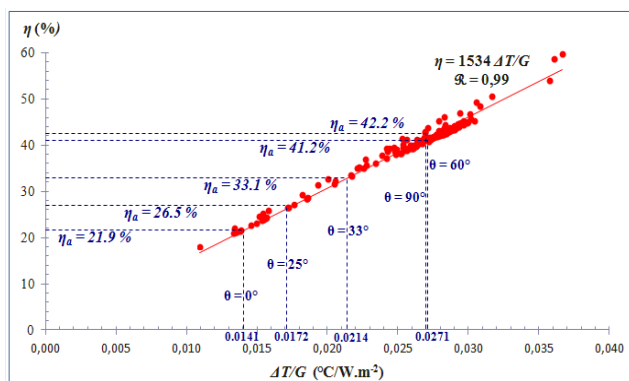
Fig. 9 illustrates the variation of η as a function of $\Delta T/G$ for the three experimental measurement series. The regression curve is linear and passes by the origin point. This regression is characteristic of the collector's behavior, whatever the tilt angle.

The relation between η and θ is not explicitly expressed in Eq. (3). Their dependence is shown in $\Delta T/G$ expression, as mentioned in section 3.3.

By introducing the mean value of $\Delta T/G$ corresponding to each tilt angle (Table 5) into the expression of the regression line ($\eta = 1534 \Delta T/G$), the efficiency average value (η_a) is obtained.

Efficiency oscillations are induced by weather conditions, especially when the solar irradiance is low as mentioned above, and also for strong variation of irradiance. The variations of η are closely related to the effect of environmental changes and the collector thermal inertia on its energy exchanges with the environment. However, all ($\eta, \Delta T/G$) points remain aligned on a regression line with a slope of $1534 \text{ m}^2 \text{ }^\circ\text{C/W}$, and a strong correlation coefficient

R of 0.99 as shown on Fig. 9.



3.5. Solar air heater performance criteria

Besides thermal efficiency and air temperature rise, solar air heater performance includes its acquisition cost, electric consumption, availability, space requirement and weight, etc. The relative importance of these criteria depends on the socio-economic environment of the operating site. For example, for domestic use, or drying agricultural products in a sunny and low-income area, acquisition cost and electric consumption are the most important criteria.

Table 6 shows the performance of the solar air heater presented in this study, with a tilt angle of 60° and under an average irradiance of 811 W/m^2 .

Table 6. Solar air heater performance

Average thermal efficiency η	41.2 %
Mean temperature rise ΔT	22 $^\circ\text{C}$
Mean thermal power P_{th}	337 W
Electrical energy $P_{elec.fan}$	23 W
Manufacturing cost C	90 €

According to these data, two performance criteria of this collector can be highlighted:

- $R1 = P_{th} / P_{elec.fan} = 14.7 \text{ [W/W]}$, which is the thermal energy produced per consumed electrical energy unit. This ratio is similar to the coefficient of performance (COP) used as a specific performance criteria for heat pumps. Thus, the COP of studied solar air heater is quite interesting compared to those of heat pumps available on the market.

- $R2 = P_{th} / C = 3.7 \text{ [W/€]}$, which is the thermal power of the air heater per monetary investment unit.

$R1$ and $R2$ constitute, in addition to η and ΔT , the main performance parameters of the studied air heater. Any

introduced modification to improve its performance is considered effective to the extent that it can increase these two parameters values, or at least maintain their initial values.

3.6. Air heater for red algae drying

Fig. 10 shows for each tilt angle θ , the mean inlet air temperature (T_{in}), the range of incident irradiance values, and minimum and maximum of the outlet air temperature.

For $\theta = 60^\circ$ allowing a better thermal efficiency of 41.2%, the outlet air temperature was in the range of 34 to 58°C, for solar irradiance between 182 and 988 W/m^2 . The use of this air heater significantly reduces the drying time of red algae *Gelidium sesquipedale* compared to the traditional drying process at approximately 28°C, which also leads to a degradation of the product quality, mainly due to possible loss of their salinity following a prolonged exposure to open air [39].

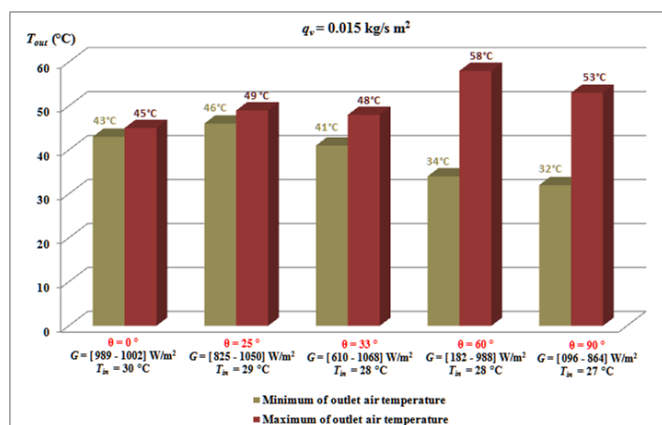


Fig. 10. Outlet air temperature for the three measurement series.

3.7. Solar potential of El Jadida

For red algae solar drying, the study of solar air heater performance is a part of the overall study which may include an evaluation of the specific solar potential of the region [40-42].

Conducted investigations [43], using an artificial neural network model (ANN) to predict annual and monthly solar irradiance maps in Morocco, show a high solar potential in El Jadida (Table 7) during the harvesting period of *Gelidium sesquipedale* (July, August and September).

Table 7. July, August, September and annual global solar irradiance on horizontal ground in El Jadida

	July	August	September	Annual
Wh/m ² /day	7080	7030	6100	5600

4. Conclusion and perspectives

The implemented solar air heater is of an affordable cost and shows an acceptable thermal performance. The main results with a constant airflow of about 0.015 $kg/s m^2$ are:

- An increase of the collector efficiency (η) and $\Delta T/G$, when the tilt angle (θ) varies from 0° to 90° . For each tilt angle corresponds a characteristic regression ($\Delta T = K_{\theta, q_v} \cdot G$) of the heater.
- For a given tilt angle, the efficiency is quasi constant.
- For a tilt angle of 60° and under an average irradiance of 811 W/m^2 during 9 hours of exposure, the harvested energy is 14.7 times the consumed electrical energy, with an efficiency of 41.2% and a temperature rise of 22 °C. The thermal power harvested per monetary unit invested is of 3.7 $W/€$.

These results can be used as a basis of dimensioning solar heaters for low temperature applications, particularly for red algae *Gelidium sesquipedale* drying. Besides the thermal performance, acquisition cost and electric consumption are important criteria to promote the use of such devices in sunny and low-income sites. These advantages should be considered for improvement of solar air heaters performance. Since the availability of the solar irradiance potential is a key part of the drying process, a fairly accurate assessment of this resource will be necessary in order to simulate the solar heater behavior along the red algae drying season.

References

- A.E. Kabeel, M.H. Hamed, Z.M. Omara and A.W. Kandeal, "Solar air heaters: Design configurations, improvement methods and applications – A detailed review", *Renewable and Sustainable Energy Reviews*, vol. 70, pp. 1189-1206, April 2017.
- E. M. Toygar, T. Bayram, O. Das, A. Demir and E.T. Turkmen, "The development and design of Solarux system with solar flat mirror and solid material high-temperature heat storage", 2nd International Conference on Renewable Energy Research and Applications (ICRERA 2013), Madrid, pp. 458-463, 20-23 October 2013.
- S. Simms and J. F. Dorville, "Thermal Performance of a hybrid photovoltaic thermal collector with a modified absorber", 4th International Conference on Renewable Energy Research and Applications (ICRERA 2015), Palermo, pp. 600-605, 22-25 November 2015.
- A. Saxena, Varun and A.A.El-Sebaili, "A thermodynamic review of solar air heaters", *Renewable and Sustainable Energy Reviews*, vol. 43, pp. 863-890, March 2015.
- T. Alam and M.H. Kim, "Performance improvement of double-pass solar air heater – A state of art of review", *Renewable and Sustainable Energy Reviews*, vol. 79, pp. 779-793, November 2017.
- A.E. Kabeel and K. Mečárik, "Shape optimization for absorber plates of solar air collectors", *Renewable Energy*, vol. 13, pp. 121-131, January 1998.
- A.A. El-Sebaili, S. Aboul-Enein, M.R.I. Ramadan, S.M. Shalaby and B.M. Moharram, "Investigation of thermal performance of double pass-flat and v-corrugated plate

- solar air heaters”, *Energy*, vol. 36, pp. 1076-1086, February 2011.
- [8] M.A Karim and M.N.A Hawlader, “Performance investigation of flat plate, v-corrugated and finned air collectors”, *Energy*, vol. 31, pp. 452-470, March 2006.
- [9] A.E. Kabeel, A. Khalil, S.M. Shalaby and M.E. Zayed, “Improvement of thermal performance of the finned plate solar air heater by using latent heat thermal storage”, *Applied Thermal Engineering*, vol. 123, pp. 546-553, August 2017.
- [10] R.K. Ravi and R. P. Saini, “Nusselt number and friction factor correlations for forced convective type counter flow solar air heater having discrete multi V shaped and staggered rib roughness on both sides of the absorber plate”, *Applied Thermal Engineering*, vol. 129, pp. 735-746, January 2018.
- [11] S. Saurav and M.M. Sahu, “Heat transfer and thermal efficiency of solar air heater having artificial Roughness: A review”, *International Journal of Renewable Energy Research*, vol. 3, pp. 498-508, June 2013.
- [12] M. Abuşka, “Energy and exergy analysis of solar air heater having new design absorber plate with conical surface”, *Applied Thermal Engineering*, vol. 131, pp. 115-124, February 2018.
- [13] N. Moumami, S. Youcef-Ali, A. Moumami and J.Y Desmons, “Energy analysis of a solar air collector with rows of fins”, *Renewable Energy*, vol. 29, pp. 2053-2064, October 2004.
- [14] B. Bhushan and R. Singh, “A review on methodology of artificial roughness used in duct of solar air heaters”, *Energy*, vol. 35, pp. 202-212, January 2010.
- [15] I.T. Türk and D. Pehlivan, “Effect of packing in the airflow passage on the performance of a solar air-heater with conical concentrator”, *Applied Thermal Engineering*, vol. 25, pp. 1349-1362, June 2005.
- [16] E.M. Languri, H. Taherian, K. Hooman and J. Reisel, “Enhanced double-pass solar air heater with and without porous medium”, *International Journal of Green Energy*, vol. 8, pp. 643-654, September 2011.
- [17] K. Rajarajeswari and A. Sreekumar, “Matrix solar air heaters – A review”, *Renewable and Sustainable Energy Reviews*, vol. 57, pp. 704-712, May 2016.
- [18] A. Ahmad, J. S. Saini and H. K. Varma, “Thermohydraulic performance of packed-bed solar air heaters”, *Energy Conversion and Management*, vol. 37, pp. 205-214, February 1996.
- [19] C. Hajjaj, A.A. Merrouni, A. Bouaichi, M. Benhmida, S. Sahnoun, A. Ghennioui and H. Zitouni, “Evaluation, comparison and experimental validation of different PV power prediction models under semi-arid climate”, *Energy Conversion and Management*, vol. 173, pp. 476-488, October 2018.
- [20] H. Amiry, M. Benhmida, R. Bendaoud, C. Hajjaj, S. Bounouar, S. Yadir, K. Raïs and M. Sidki, “Design and implementation of a photovoltaic IV curve tracer: Solar modules characterization under real operating conditions”, *Energy Conversion and Management*, vol. 169, pp. 206-216, May 2018.
- [21] C. Hajjaj, A.A. Merrouni, A. Bouaichi, M. Benhmida, B. Ikken, S. Sahnoun, A. Ghennioui, A. Benlarabi and H. Zitouni, “Evaluation of Different PV Prediction Models. Comparison and Experimental Validation with One-Year Measurements at Ground Level”, *International Conference on Electronic Engineering and Renewable Energy*, Saidia, pp. 617-622, 15-17 April 2019.
- [22] C. Hajjaj, B. Abdellatif, A.M. Ahmed, B. Mohammadi, B. Amin, G. Abdellatif, Z. Houssain and I. Badr, “Experimental Validation of Non-Linear Empirical Model to Simulate the Photovoltaic Production Under Semi-Arid Climate. Case Study of Benguerir, Morocco”, *International Conference on Photovoltaic Science and Technologies*, Ankara, pp. 1-5, 4-6 July 2018.
- [23] C. Hajjaj, H. Amiry, R. Bendaoud, S. Yadir, A. Elhassnaoui, S. Sahnoun, M. Benhmida and A. EL Rhassouli, “Design of a New Photovoltaic Panel Cooling System to Optimize its Electrical Efficiency”, *International Renewable and Sustainable Energy Conference*, Marrakech, pp. 623-627, 14 – 17 November 2016.
- [24] N. Hanif, M. Chair, M. C. Idrissi and T. Naoki, “The exploitation of Gelidium red algae in the region of El-Jadida”, *Afrique Science*, vol. 10, pp. 103-126, 2014.
- [25] H.J. Bixler, H. Porse, “A Decade of Change in the Seaweed Hydrocolloids Industry”, *Journal of Applied Phycology*, vol. 23, pp. 321- 335, May 2010.
- [26] A. M. Givernaud, L. A. Hassani, T. Givernaud, Y. Lemoine, O. Benharbet, “Biology and agar composition of Gelidium sesquipedale harvested along the Atlantic coast of Morocco”, *Hydrobiologia*, vol. 398, pp. 391-395, April 1999.
- [27] R. Pérez, *Ces algues qui nous entourent: Conception actuelle, rôle dans la biosphère, utilisations, culture*, 1st ed., Quae: France 2009, pp. 1-272.
- [28] A. Nussinovitch, *Hydrocolloid applications: gum technology in the food and other industries*, 1st ed., Blackie Academic and Professional: New York 1997, pp. 1-338.
- [29] S.G. Lardiere, *Structural analysis of the sulphated water-soluble cell-wall polysaccharides from the gametic stages of the red seaweed Asparagopsis armata Harvey (Rhodophyta, Bonnemaisoniaceae)*, Ph.D. thesis, University OF western Brittany, 2004.
- [30] A. Nussinovitch, *Polymer Macro- and Micro-Gel Beads: Fundamentals and Applications*, 1st ed., Springer: New York 2010, pp. 1-278.
- [31] A. El-abidi, S. Yadir, F. Chanaa, M. Benhmida, H. Amiry, H. Ezzaki and H. Bousseta, “Modeling and simulation of a modified solar air heater destined to drying the Gelidium Sesquipedale”, *International Journal of Renewable Energy Research*, vol.8, pp. 2003-2013, December 2018.
- [32] F. Dupriez, *Détermination du débit des fluides par intégration du champ des vitesses*, Techniques de l’Ingénieur: France 1992.
- [33] A.E. Kabeel, M.H. Hamed, Z.M. Omara and A.W. Kandeal, “Influence of fin height on the performance of a glazed and bladed entrance single-pass solar air heater”, *Solar Energy*, vol. 162, pp. 410-419, March 2018.
- [34] F. Chabane, N. Moumami and S. Benramache, “Experimental study of heat transfer and thermal performance with longitudinal fins of solar air heater”,

- Journal of Advanced Research*, vol.5, pp.183-192, April 2013.
- [35] F. Chabane, N. Moumami, S. Benramache and A.S. Tolba, “ Experimental study of heat transfer and an effect the tilt angle with variation of the mass flow rates on the solar air heater”, *International Journal of Science and Engineering Investigations*, vol. 1, pp. 61-65, January 2012.
- [36] D. Jain and R.K. Jain, “Performance evaluation of an inclined multi-pass solar air heater with in-built thermal storage on deep-bed drying application”, *Journal of Food Engineering*, vol. 65, pp. 497-509, December 2004.
- [37] D. Alta, E. Bilgili, C. Ertekin and O.Yaldiz, “Experimental investigation of three different solar air heaters: Energy and exergy analyses”, *Applied Energy*, vol. 87, pp. 2953-2973, October 2010.
- [38] F. Chabane, N. Moumami, A. Brima and S. Benramache, “Thermal efficiency analysis of a single-flow solar air heater with different mass flow rates in a smooth plate”, *Frontiers in Heat and Mass Transfer*, vol. 4, pp 1-6, May 2013.
- [39] M. Kumar, S.K. Sansaniwal and P. Khatak, “Progress in solar dryers for drying various commodities”, *Renewable and Sustainable Energy Reviews*, vol. 55, pp. 346-360, March 2016.
- [40] Y. Mehmet, C. Medine and B. Ramazan, “A review of data mining and solar power prediction”, 5th International Conference on Renewable Energy Research and Applications (ICRERA 2016), Birmingham, pp. 1117-1121, 20-23 November 2016.
- [41] A. Rami, A. Ali and F.M. Mohamad, “A predictive evaluation of global solar radiation using recurrent neural models and weather data”, 6th International Conference on Renewable Energy Research and Applications (ICRERA 2017), San Diego, pp. 195-199 , 5-8 November 2017.
- [42] D. Mehmet, Y. Mehmet, S. Seref and C. Ilhami, “Prediction of solar radiation using meteorological data”, 1st International Conference on Renewable Energy Research and Applications (ICRERA 2012), Nagasaki, pp. 1-4, 11-14 November 2012.
- [43] A. Ouammi, D. Zejli, H. Dagdougui, R. Benchrifa, “Artificial neural network analysis of Moroccan solar potential”, *Renewable and Sustainable Energy Reviews*, vol. 16, pp. 4876-4889, June 2012.